Progress on the ICRF orbit-averaged quasilinear operator of TORIC full-wave code

R. Bilato, V. Belmondo, M. Brambilla, O. Maj, E. Poli

Max-Planck Institut für Plasmaphysik - Germany, EURATOM Ass.

Introduction

Several full-wave codes have been interfaced with Fokker-Planck (FP) solvers to model consistently propagation and absorption of radio-frequency (RF) waves in the ion-cyclotron (IC) range of frequencies. In many studies, the solution of either the surface-averaged or the zero-orbit-width averaged FP equations can be considered adequate to describe the back-reaction of ICRF heating on the wave propagation and absorption. This, however, is not the case for those problems where the fate of very energetic ions produced with ICRF waves matters the most, e.g. drive of MHD activity. Because of their large radial excursions, these ions can explore large portions of the plasma column, figure 1, as well as experience large Doppler shifts in the resonance with waves. To properly describe the interaction of energetic particles with RF waves, one has to solve the orbit-averaged FP equation, where the ICRF contribution enters as an orbit-averaged quasilinear diffusion operator (QDO).

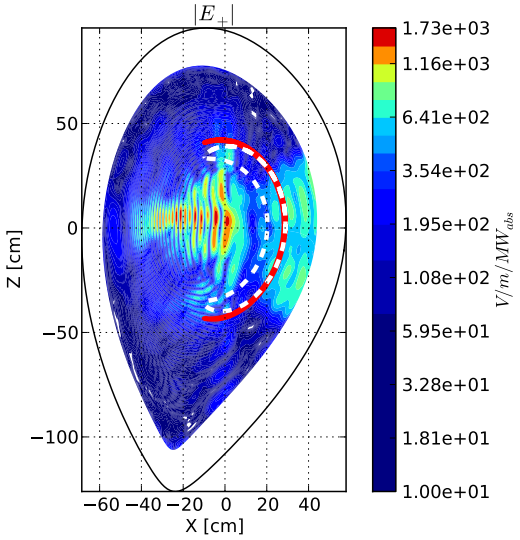

Figure 1: *Orbits of co-passing trapped particles with energy of 1 keV (red) and 100 keV (white). The background is the module of the clockwise rotating components of the wave electric field. These orbits are evaluated with the guiding-center solver of the* `TORIC` *code.*

In the following, after a sketch of the derivation of QDO added in the `TORIC-SSFPQL` package [1], an estimate of the heating rate derived by such an operator is compared with the equivalent quantity calculated by `SSFPQL`, which assumes zero-orbit with approximation.

Orbit-averaged quasilinear operator

The large time-scale separation between the wave period ($T_\omega = 2\pi/\omega$, with ω the angular wave frequencies) and the characteristic thermal equilibration times justifies splitting the distribution function in a slow, f_0, and a fast, f_1, components, the latter evolving in the short T_ω time-scale. The pertinent quasilinear coupled equations for f_0 and f_1 are

$$\begin{aligned} \frac{\partial f_0}{\partial t} + \boldsymbol{v}\cdot\nabla_{\boldsymbol{x}} f_0 + \boldsymbol{a}_0\cdot\nabla_{\boldsymbol{v}} f_0 &= \nabla_{\boldsymbol{v}}\cdot\boldsymbol{\Gamma}_c(f_0) - \nabla_{\boldsymbol{v}}\cdot\langle \boldsymbol{a}_1 f_1\rangle_\omega \\ \frac{\partial f_1}{\partial t} + \boldsymbol{v}\cdot\nabla_{\boldsymbol{x}} f_1 + \boldsymbol{a}_0\cdot\nabla_{\boldsymbol{v}} f_1 &= -\boldsymbol{a}_1\cdot\nabla_{\boldsymbol{v}} f_0 \end{aligned} \tag{1}$$

where $\mathbf{\Gamma}_c$ is the collisional flux in velocity, $\langle\cdots\rangle_\omega$ stands for the time average over a wave period T_ω, and $\boldsymbol{a}$ is the acceleration due to the Lorentz force, split in its contributions from the confining em fields, $\boldsymbol{a}_0$, and from the RF fields, $\boldsymbol{a}_1$. By integrating the second equation along the unperturbed orbits, one obtains the *formal* solution f_1 to plug in the last term of the first equation, which is the QLO describing the wave-particle interaction in the time evolution of f_0. To perform the orbit average, a convenient coordinate system is built with a set of constants of the unperturbed motion, $\boldsymbol{I}$, completed with a set of angles $\boldsymbol{\theta}$ [2]. The QLO can be written as $Q(f_0) = \mathscr{J}^{-1}\partial_{I^i}\left(\mathscr{J}\, Q^{ij}\partial_{I^j} f_0\right)$ with $\mathscr{J}$ the Jacobian of the coordinate systems and

$$Q_w^{ij} = \frac{1}{2}\mathrm{Re}\left\{\sum_{\kappa_{1,2}}\sum_n\sum_{\substack{m_1\\m_2}} e^{-\mathrm{i}\boldsymbol{k}_1\cdot\boldsymbol{r}}\,\nabla_{\boldsymbol{v}} I^i\cdot\boldsymbol{a}^*_{1,\omega,\boldsymbol{k}_1}\int_{-\infty}^{t} e^{\mathrm{i}[\boldsymbol{k}_2\cdot\boldsymbol{r}'-\omega(t'-t)]}\,\nabla_{\boldsymbol{v}'} I^j\cdot\boldsymbol{a}'_{1,\omega,\boldsymbol{k}_2}\,\mathrm{d}t'\right\} \tag{2}$$

Here the chosen set of invariants of the unperturbed motion is $\boldsymbol{I} = (\mu, \varepsilon, P_\varphi)$, with μ the magnetic momentum, ε the particle energy, and P_φ the toroidal canonical momentum, whereas the angles are $\boldsymbol{\theta} = (\phi_v, \vartheta, \varphi)$, with ϕ_v and φ the gyro– and toroidal angles, respectively, and ϑ the poloidal angle associated with the bouncing motion. In (2) the spectral ansatzt of the wave-fields is assumed (κ, m, n are respectively the radial, poloidal and toroidal components of the wavevectors) and the axisymmetry is used to remove one of the sum over n. In $(\boldsymbol{\theta},\boldsymbol{I})$ coordinates the orbit average is simply the average over the angles $\boldsymbol{\theta}$, and the equation for the orbit-averaged distribution function, $\bar{f}_0(\boldsymbol{I})$ (the bar over the symbols stands for the orbit-average), is

$$\partial_t \bar{f}_0 = \frac{1}{\bar{\mathscr{J}}}\,\frac{\partial}{\partial I^i}\left[\bar{\mathscr{J}}\left(\bar{F}^i_{\mathrm{cl}}\bar{f}_0 + \bar{D}^{ij}_{\mathrm{cl}}\,\frac{\partial \bar{f}_0}{\partial I^j}\right)\right] + \frac{1}{\bar{\mathscr{J}}}\,\frac{\partial}{\partial I^i}\left[\bar{\mathscr{J}}\;\bar{Q}^{ij}_w\,\frac{\partial \bar{f}_0}{\partial I^j}\right] \tag{3}$$

where the collisional flux is written in terms of its friction and diffusion components, $\bar{\boldsymbol{F}}_{\mathrm{cl}}$ and $\bar{\boldsymbol{D}}_{\mathrm{cl}}$ respectively. The $\boldsymbol{\theta}$–average of the convective terms in (3) is zero because of the Liouville theorem, and of $\partial\mathscr{J}/\partial t$, $\dot{\boldsymbol{I}} = 0$. In deriving (3), the contribution dependent on the difference $\left(f_0(\boldsymbol{\theta},\boldsymbol{I}) - \bar{f}_0(\boldsymbol{I})\right)$ has been neglected by assuming that for times long enough f_0 approaches $\bar{f}_0$. After some algebra the expression of $\bar{Q}^{ij}_w$ added to `TORIC` can be stylized as

$$\bar{\mathscr{J}}\,\bar{Q}^{ij}_w = \frac{1}{2}\mathrm{Re}\left\{\sum_{\kappa_{1,2}}\sum_{\substack{n\\m_{1,2}}}\sum_{p=0}^{\infty}\sum_{\tau^{\mathrm{res}}_{p,\boldsymbol{k}_2}}\left(e^{\mathrm{i}\boldsymbol{k}_1\cdot\boldsymbol{R}_g}\,|\mathscr{T}_{\mathrm{res}}|\,\Delta^i_{p,\boldsymbol{k}_1}\right)^*_{\tau^{\mathrm{res}}_{p,\boldsymbol{k}_2}}\left(e^{\mathrm{i}\boldsymbol{k}_2\cdot\boldsymbol{R}_g}\,|\mathscr{T}_{\mathrm{res}}|\Delta^j_{p,\boldsymbol{k}_2}\right)_{\tau^{\mathrm{res}}_{p,\boldsymbol{k}_2}}\right\} \tag{4}$$

where: $\boldsymbol{R}_g$ is the guiding-center position, p is the IC harmonic index, $\Delta^i_{p,\boldsymbol{k}}$ depends on the wave fields and contains the usual Bessel functions of argument $k_\perp v_\perp/\Omega_c$ [3], and $\mathscr{T}_{\mathrm{res}}$ is the resonance kernel. Because of the highly-oscillatory nature of the exponential in (2), there are finite contributions only at times when its phase is stationary, $\tau^{\mathrm{res}}_{p,\boldsymbol{k}_2}$, which dependent only on $\boldsymbol{k}_2$ of the solution of the Vlasov equation. In matrix form, Eq. (4) can be written as $\bar{\boldsymbol{Q}} = \boldsymbol{A}^\dagger\boldsymbol{A}$, which implies that $\bar{\boldsymbol{Q}}$ is definite *non*–negative. This property is fulfilled in the implementation of (4) in `TORIC`. The form of the resonance weight $|\mathscr{T}_{\mathrm{res}}|$ is the key issue, both conceptually and

technically, in deriving (4): It is analytically known in the asymptotic limit of *decorrelated* (stationary phase approximation) and strongly *correlated* (Airy functions) passages through near consecutive resonances. An approximated analytical transition between these two asymptotic solutions is viable when accounting for the decorrelation of the wave-particle phase, as done by Catto and Myra [4]. Their function $\mathscr{C}(x,\eta)$ is shown in figure 2 for different values of the decorrelation parameter η, and it has been extended [5] as $|\mathscr{T}_{\rm res}(\tau)|^2 = 2\sqrt{\pi}\mathscr{C}(g(\tau))$ with

$$g(\tau) = \begin{cases} -|\ddot{\chi}_{p,\boldsymbol{k}}(\tau)|^2, & \text{for } \ddot{\chi}_{p,\boldsymbol{k}}(\tau) \neq 0, \\ \left| \dfrac{\dot{\chi}_{p,\boldsymbol{k}}(\tau)}{\left(\dddot{\chi}_{p,\boldsymbol{k}}(\tau)/2\right)^{1/3}} \right|, & \text{for } \ddot{\chi}_{p,\boldsymbol{k}}(\tau) = 0, \end{cases}$$

where: $\dot{\chi} = k_{\|}v_{\|} + p\Omega_{\rm c} + \boldsymbol{v}_D \cdot \boldsymbol{k} - \omega$, ($\boldsymbol{v}_D$ the particle drift velocity), $\tau_{\rm sp}$ are the decorrelated resonances, $\dot{\chi}(\tau_{\rm sp}) = 0$, and $\tau_{\rm tg}$ are points between two merging resonances.

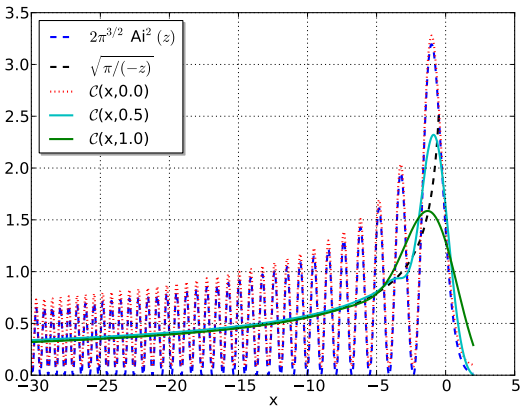

Figure 2: *Catto-Myra function for different values of the decorrelation parameter η. Black dashed line shows the stationary-phase approximation whereas the blue dashed line the Airy function.*

Discussion

In the case of energetic ions the IC resonances can be substantially displaced with respect to the resonance layer $\omega \approx \Omega_c$ (fig. 1). This has an impact on the amplitude of the wave-particle interaction, since the wave fields can considerably vary, especially close to the ion-ion and IC fundamental resonances. Additionally, the travel time of the particles changes along the orbit and thus also the resonance time. To account properly for these effects, the particle orbits have to be calculated and the resonance positions with the Fourier modes of wave fields have to be identified [6]. To numerical evaluate (4), the wave fields of `TORIC` are directly used. Figure 3.left shows an example of $Q^{\varepsilon\varepsilon}$ normalized to ε^2 as function of $\Lambda_{\rm eq} = \mu B_{\rm eq}/\varepsilon$, with $B_{\rm eq}$ the B value at the starting obit point on the midplane. Since Δ^{ε} is proportional to $v_{\perp} \propto \Lambda_{\rm eq}^{1/2}$, $Q^{\varepsilon\varepsilon}$ increases proportionally with $\Lambda_{\rm eq}$. However, at the transition between passing and trapped particles ($\Lambda_{\rm eq} \approx 0.8$), $Q^{\varepsilon\varepsilon}$ drops, since the turning points of the orbits, where the particle stay longer, do not necessarily coincide with the resonance points. For ions with higher $\Lambda_{\rm eq}$ (about 0.9) the turning points are close to the IC resonance and $Q^{\varepsilon\varepsilon}$ reaches its maximum. Additionally, a trapped ion can have a maximum number of four resonances with the same wave mode, which reduces to two for passing particles. This topological change of the wave-particle interaction also contributes to higher $Q^{\varepsilon\varepsilon}$ values for trapped resonating ions.

As preliminary check of the quasilinear operator, the quasilinear heating rate is considered

$$P_{\rm RF}(\psi) = \frac{1}{\Delta V}\int \varepsilon \frac{1}{\bar{\mathscr{J}}}\frac{\partial}{\partial I^i}\left(\bar{\mathscr{J}}\bar{Q}^{ij}_{\rm w}\frac{\partial \bar{f}_0}{\partial I^j}\right)\bar{\mathscr{J}}\,{\rm d}\boldsymbol{I} = \frac{n_i(\psi)}{T_i(\psi)}\int_0^{\varepsilon_{\rm max}} {\rm d}\varepsilon \int_0^1 {\rm d}\Lambda_{\rm eq}\,\bar{\mathscr{J}}\,\bar{Q}^{\varepsilon\varepsilon}_{w}\,\frac{e^{-\varepsilon/T_i}}{f_n} \quad (5)$$

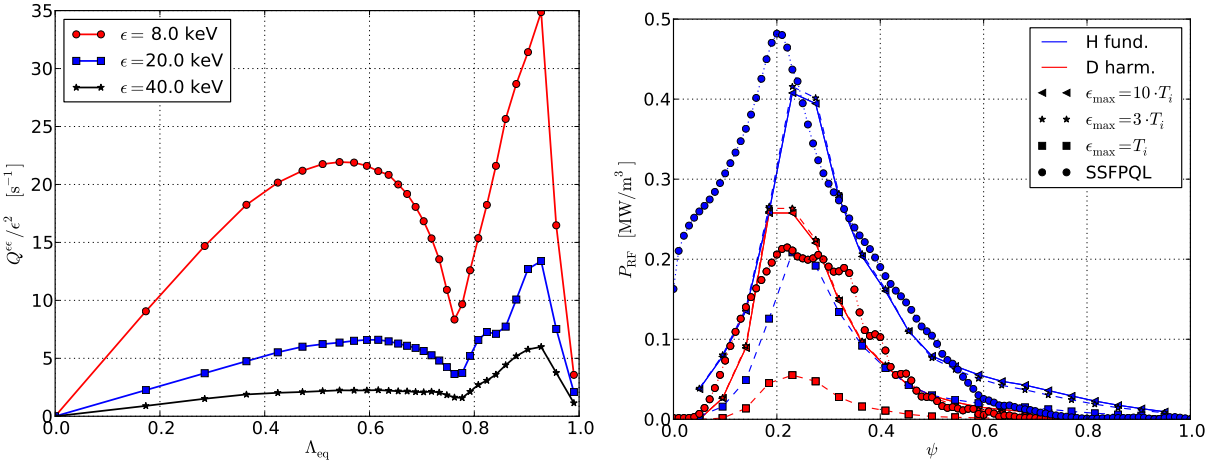

Figure 3: *(left)* $Q^{\varepsilon\varepsilon}/\varepsilon^2$ *as function of* Λ_{eq} *for three values of the particle energy and at* $\psi = 0.6$. *(right) Profiles of the absorbed power by the minority H (fundamental) and by the majority D (first harmonic) calculated with (5) (triangles, squares and stars) are compared with* `SSFPQL` *results (bullets).*

where: $P_\varphi \approx \psi$ is assumed for comparison with `SSFPQL`; $n_i(\psi)$ and $T_i(\psi)$ are the plasma density and temperature of the resonating ion species, and f_N is the normalization constant of the Maxwellian in these coordinates. The last equality amounts to approximating $\bar{f}_0$ with the Maxwellian in the absence of the solution of the quasilinear equation for f_0. Figure 3.right shows the profiles of the absorbed power for three different energy cuts, ε_{max}, in (5). Already at ε_{max} equal to three times the local thermal energy T_i (stars) the profiles converge to the final ones (squares). Thus, at least for the profiles of the absorbed power the thermal bulk plays the main role in ICRF heating simulations. Because of the completely different models, the comparison with the absorption profiles calculated with `SSFPQL` can only be very qualitative. First, in figure 3.right (5) predicts broader profiles on the outer part of the plasma column. This is only partially due to the finite orbit-width effects, since it holds also for moderate energies, $\varepsilon_{max} = 3\,T_i$. In the region between the magnetic axis and the IC resonance, $\omega = \Omega_c$ (at $\psi \approx 0.2$ in this case), the profiles predicted by (5) are narrower. Finally, the power redistribution between hydrogen (minority, resonating at the fundamental) and deuterium (majority, resonating at the first harmonic) is different. These discrepancies are likely due to the different description of the wave-particle interaction in `SSFPQL` and in (5), more accurate in the latter, and of the use of the Maxwellian in (5), a too rough approximation of the FP solution. Nevertheless, the order-of-magnitude agreement is a positive first test of QLO added to the `TORIC` code.

References

[1] BRAMBILLA, M. and BILATO, R., Nuclear Fusion **49** (2009) 085004.

[2] ERIKSSON, L.-G. and HELANDER, P., Physics of Plasmas **1** (1994) 308.

[3] BRAMBILLA, M., Nuclear Fusion **47** (2007) 175.

[4] CATTO, P. J. and MYRA, J. R., Physics of Fluids B: Plasma Physics **4** (1992) 187.

[5] BILATO, R. and BRAMBILLA, M., AIP Conference Proceedings **1580** (2014) 306.

[6] BELMONDO, V., BILATO, R., BRAMBILLA, M., and MAJ, O., Journal of Physics: Conference Series **260** (2010) 012001.